Study on voltage coordination optimization of microgrid with electric vehicle load response

Zhengjie Luo[1], Hui Ren[1], Guoyu Xin[2], Mingkuo Xu[1], and Fei Wang[3]

[1]North China Electric Power University - Baoding Campus
[2]State Grid Hebei Electric Power Company
[3]North China Electric Power University

April 7, 2023

Abstract

The aggregation of the remaining battery capacity of EVs can be used as distributed energy storage to participate in electricity market auxiliary services in the form of V2G, however, their reliability is affected by the uncertainty of EV travel. In this paper, we consider the uncertainty of EV load response and propose a resolution method for quantifying the reliability of EV aggregation capacity in the day-ahead market. The paper first classifies EV users by analyzing historical charging data. Secondly, based on the composite Poisson process, the V2G capacity and reliability model for the aggregator's participation in the day-ahead auxiliary service bidding are proposed and validated using actual data. Based on this model, aggregators can decide the power of V2G bidding for any time slot on day t+1 according to the reliability requirements of the standby market for the standby capacity contracted before that day. Finally, this paper organically combines PV and EV aggregators in the microgrid and uses genetic algorithms to optimize the simulation of the microgrid voltage operation state under different scenarios in the IEEE 33-node system. The results show the effectiveness of the coordinated optimization scheme of PV and EV clusters for the optimization of microgrid voltage.

Hosted file

Study on voltage coordination optimization of microgrid with electric vehicle load response.docx available at https://authorea.com/users/604006/articles/634127-study-on-voltage-coordination-optimization-of-microgrid-with-electric-vehicle-load-response

1

Manuscript Details

1. Article Title

Study on voltage coordination optimization of microgrid with electric vehicle load response

2. Running Head

Microgrid Voltage Optimization Based on EVA Reliability Model

3. Order of Authors

Zhengjie Luo [1], Hui Ren [1*], Guoyu Xin [2,1], Mingkuo Xu [1], Fei Wang [1]

4. Author's Contribution

Conceptualization, H.R. and F.W.;
Formal Analysis, Z.L.;
Resources, Z.L. and G.X.;
Software, Z.L. and G.X.;
Supervision, H.R. and F.W.;
Visualization, Z.L.;
Writing - Original Draft, Z.L., H.R., G.X. and M.X.;
Writing - Review & Editing, Z.L., H.R. and M.X.

5. Affiliation of All Authors

1 Department of electrical engineering, North China Electric Power University, 071003, Baoding, China
2 State Grid Hebei Electric Power Co., Ltd. Hengshui Power Supply Company, 053000, Hengshui, China

6. Postal and E-mail Address of the Corresponding Author

E-mail Address: hren@ncepu.edu.cn, dahui.ren@outlook.com
Postal Address: 619 North Yonghua Street, Baoding 071003, China

7. Funding Information

None

8. Conflict of Interest statement

The authors declare that they have no known competing financial interests or personal relationships that could have appeared to influence the work reported in this paper.

9. Permission to reproduce materials from other sources

None

10. Data Availability statement.

The data that support the findings of this study are available from the corresponding author upon reasonable request.

11. ORCID

Zhengjie Luo   0009-0003-6705-3924

12. Article type

Original Research Paper

Abstract

The aggregation of the remaining battery capacity of EVs can be used as distributed energy storage to participate in electricity market auxiliary services in the form of V2G, however, their reliability is affected by the uncertainty of EV travel. In this paper, we consider the uncertainty of EV load response and propose a resolution method for quantifying the reliability of EV aggregation capacity in the day-ahead market. The paper first classifies EV users by analyzing historical charging data. Secondly, based on the composite Poisson process, the V2G capacity and reliability model for the aggregator's participation in the day-ahead auxiliary service bidding are proposed and validated using actual data. Based on this model, aggregators can decide the power of V2G bidding for any time slot on day t+1 according to the reliability requirements of the standby market for the standby capacity contracted before that day. Finally, this paper organically combines PV and EV aggregators in the microgrid and uses genetic algorithms to optimize the simulation of the microgrid voltage operation state under different scenarios in the IEEE 33-node system. The results

show the effectiveness of the coordinated optimization scheme of PV and EV clusters for the optimization of microgrid voltage.

Please see the next page for the main text file.

Study on voltage coordination optimization of microgrid with electric vehicle load response

Zhengjie Luo [1], Hui Ren [1*], Guoyu Xin [2,1], Mingkuo Xu [1], Fei Wang [1]

[1] Department of electrical engineering, North China Electric Power University, 071003, Baoding, China
[2] State Grid Hebei Electric Power Co., Ltd. Hengshui Power Supply Company, 053000, Hengshui, China
*hren@ncepu.edu.cn

Abstract: The aggregation of the remaining battery capacity of EVs can be used as distributed energy storage to participate in electricity market auxiliary services in the form of V2G, however, their reliability is affected by the uncertainty of EV travel. In this paper, we consider the uncertainty of EV load response and propose a resolution method for quantifying the reliability of EV aggregation capacity in the day-ahead market. The paper first classifies EV users by analyzing historical charging data. Secondly, based on the composite Poisson process, the V2G capacity and reliability model for the aggregator's participation in the day-ahead auxiliary service bidding are proposed and validated using actual data. Based on this model, aggregators can decide the power of V2G bidding for any time slot on day t+1 according to the reliability requirements of the standby market for the standby capacity contracted before that day. Finally, this paper organically combines PV and EV aggregators in the microgrid and uses genetic algorithms to optimize the simulation of the microgrid voltage operation state under different scenarios in the IEEE 33-node system. The results show the effectiveness of the coordinated optimization scheme of PV and EV clusters for the optimization of microgrid voltage.
Keywords: electric vehicle; V2G; aggregator; hybrid Gaussian distribution; genetic algorithm; voltage optimization

1. Introduction

This document is a template, an electronic copy of which can be downloaded from the Research Journals Author Guide page on the IET's Digital Library. For questions on paper guidelines, please contact the relevant journal inbox as indicated on each journal's website.

Before submitting your final paper, check that the format conforms to this template and the Author Guide [1]. Specifically, check to make sure that the correct referencing style has been used and the citations are in numerical order throughout the text. If your paper does not meet all of the requirements, your paper will be unsubmitted and you will be asked to correct it.

In the new energy system, due to the uncertainty of the new energy output such as scenery, the voltage operation state of the distribution network is disturbed, which requires multiple renewable energy sources to coordinate and complement each other to ensure the stability, safety and economy of the distribution network operation. Although the traditional voltage regulation can solve the problem of excessive voltage deviation, but the economy is poor. A large amount of research data shows the feasibility of the voltage stability optimization method combining distributed energy storage with wind power and PV power generation [1]. As a type of distributed energy storage resource, the ownership of electric vehicles (EVs) is increasing year by year, and the percentage of parking time in their overall operation process is up to more than 90% [2], and the remaining charging and discharging capacity of a large number of electric vehicle (EV) batteries can be aggregated to participate in electricity market auxiliary services [3] [4] [5]. The full mobilization of all types of electric vehicles in auxiliary services helps to reduce the load pressure on the grid and regulate the voltage at critical nodes [6]. However, as a distributed energy storage resource, the capacity of EV is affected by the travel of EV

users and has greater uncertainty compared with conventional distributed energy storage. After EV clusters are handed over to the grid dispatch centre for management, the reliability of their bidding power at each moment directly affects the grid dispatch centre in arranging the day-ahead dispatch plan as well as their participation in auxiliary services, and the participation of EV clusters in standby services must be guaranteed to have sufficiently high reliability [7]. Under the current market mechanism, participation in different standby services has different bidding lead times and different reliability requirements. Taking the participation of AGC units in frequency regulation as an example, the regulation amount accuracy requirement of AGC units is 3%. There are few studies on the accuracy or reliability requirements for EV cluster participation in standby, and the reliability index for EV cluster participation in V2G is set to 0.95 in the literature [8]. The uncertainty of EV users due to their travel time and travel purpose leads to uncertainty in whether EV users can participate in V2G at any time slot and the amount of V2G power that can be released after participation. Therefore, it is necessary to study the method of quantifying the reliability of EV cluster participation in V2G and its influencing factors, so that EVA can determine the type and number of contracted EV users, the type of backup services to be participated, and the amount of electricity to be tendered in accordance with the reliability requirements. The literature [9] considers the uncertainty of the scenic power output and constructs a multi-scenario hybrid energy storage optimal allocation model considering the complementary advantages of multiple flexible resources to optimize the flexible power supply in the new power system. In the literature [10], a distribution network model prediction control method is proposed to establish a distribution network voltage optimization model for the problem of frequent voltage fluctuations in the distribution network due to the extensive access of distributed energy sources. In distribution systems, the voltage is
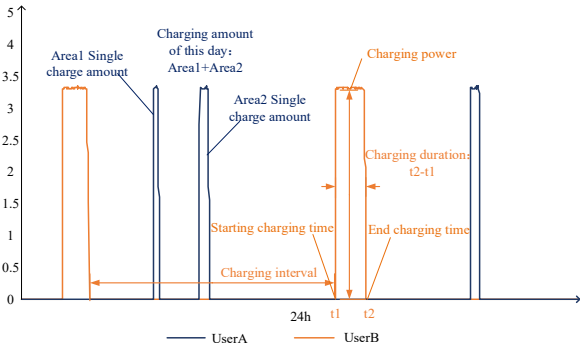
Figure 1 *48-hour charging curve for any two EV users*

generally regulated by reactive power, but since low- and medium-voltage distribution networks possess a high impedance ratio, the impact of active currents on voltage is more significant compared to reactive power [11-13]. Today, with the wide access of distributed energy sources, active power becomes the key to influence its voltage level and tidal current distribution [14], therefore, this paper mainly considers the active output of electric vehicle aggregators in the microgrid system. The literature [15] clarifies that with the widespread access to distributed generation and EVs, it has led to significant changes in the structure, function and operational characteristics of the grid, and proposes a control and management approach for distributed generation and EVs by the power system operator. The literature [16-17] improves the reliability of power reserves by guiding EV charging and discharging behaviour through peak and valley tariffs as well as dynamic tariffs to achieve the ability to provide backup to the system, but the reliability of EV participation in V2G is not mentioned in the paper. In terms of system voltage control and reduction of network losses, the high penetration of new energy systems makes the voltage fluctuations in the distribution network more severe. In new energy systems, reactive power from static compensation devices or PV and active power provided by EVAs can be used to reduce network losses and voltage fluctuations [18]. The literature [19] considered the stochastic nature of EV behaviour and the uncertainty of power output, and used a deep learning approach to verify that EVs can effectively reduce power fluctuations. The literature [20] considered the future information of EV clusters and the willingness of EV users to participate in auxiliary services, and proposed a long- and short-term neural network-based method to predict the backup capacity of EV clusters. Therefore, the voltage regulation of distribution network by participating in V2G after EV aggregation has a broad prospect and its potential is worthy of deeper exploration and full use.

The main research work of this paper is as follows: in Section I, EV historical charging data and EV user classification method are introduced; Section II proposes an EVA V2G-capable capacity calculation method and EVA reliability model based on compound Poisson distribution; Section III introduces a microgrid voltage optimization model for PV and EV coordination and runs optimization in IEEE 33-node system by genetic algorithm; Section IV Section 5 presents the microgrid voltage optimization simulation with EV load response, and finally, the microgrid economics and EVA economics are also presented; Section 6 is the conclusion section, which summarizes the reliability

simulation effect of EVA participation in auxiliary services and the microgrid voltage optimization effect.

2. EV charging characteristics and classification based on EV historical data

The daily charging volume of EV users and the charming cycle show that EV batteries have a certain residual capacity in addition to their daily driving power consumption. Therefore, if EV users are fully charged daily during low tariff hours such as early morning, the remaining power can be aggregated by EVA to provide maximum power to the grid and participate in standby service when needed, after removing their daytime driving power consumption.

Figure 1 shows the charging profiles of any two users in the dataset provided by Pecan Street Inc. over a 48-hour period [21]. The following two EV users, both of which have a battery capacity of 54 kWh, can be seen from Figure 1 that the two different EV users differ in terms of charging period, charging interval, amount per charge, and daily charging volume. Then, different EV users have different ability to participate in standby service.

This paper analyses the electricity consumption habits of EV users based on existing studies [22][23]. And the users daily charging expectation, starting charging period and charging interval are used as characteristic labels to classify the users. This section also selects the main characteristic behaviours of EV users as follows: habitual charge periods T_{habit}, desired charge interval $EXP(In)$, desired charge value $\overline{Q_d}$, etc. The behavioural characteristics of EV users are extracted from the historical charging data of EV users, and EV users are classified into three categories based on the characteristics: short-range commuters, long-range commuters, and residential users. By classifying users, the impact of each category of users on the bidding value and delivery reliability of EVs participating in V2G at different time slots is further quantified.

3. V2G reliability model for EV clusters

In this paper, it is assumed that the EV users enter into a V2G ancillary service contract with EVA. The information and energy exchange relationship between the grid dispatch centre, EVA, and EV cluster is shown in Figure 2 [24]. EVA submits the V2G bidding value to the grid dispatch centre 24 hours in advance, and dispatches the contractable EVs to participate in V2G when the execution time slot arrives. When the contracted EV is in the driving state at that time slot, it is assumed that it cannot participate in V2G according to the contract; when it is in the parked state, it is assumed that it fulfills the contract to participate in V2G.

Due to the time lead time requirement for standby service bidding and the uncertainty of EV, when there are
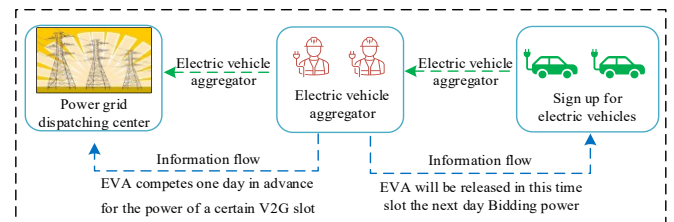

Figure 2 *Upper power grid, EV aggregator, EV cluster information and energy interaction diagram*

more default EV users or when EVA bids for higher power, it will lead to the risk of not being able to fulfill the agreed power when EVA delivers the standby capacity in real time, resulting in EVA will be penalized by the grid and even affect grid security. If the EVA contracted V2G capacity before the day is conservative, the reliability of delivery by contract is improved. However, it also affects the revenue of EVA and EV users, and affects the motivation of EV users to sign the contract, leading to the waste of flexible resources.

Considering the daily electricity available for each EV customer to join in V2G as a random variable, combined with the compound Poisson distribution, the reliability model of EVA participation in V2G can be defined as follows.

3.1. Compound Poisson Distribution

A Compound Poisson distribution means that when events that follow a Poisson process occur, each event is accompanied by a random variable (e.g., economic loss, equipment loss, etc.). The number of events $N(t)$ in time $(0, t)$ is known to be a Poisson process with ratio λ. Let the random variable V_i be associated with the failure event i ($i=1, 2, 3, \ldots$). The variable V_i is the significant fault associated with the fault i (e.g., the economic loss due to fault i). Assume that the variable $V_1, V_2, \ldots, V_n$ are an independent random variable. That is:

The significant fault accumulated at the tth time slot is:

$$Z(t) = \sum_{i=1}^{N(t)} V_i, t \geq 0 \qquad (1)$$

The process $Z(t), t \geq 0$ is said to be a Compound Poisson process.

Assume that all important faults V_i are positive, for V_i:

$$P_r(V_i \geq 0) = 1 \qquad (2)$$

Assume the threshold value of the critical fault accumulation value as C, if $Z(t) > C$, then the whole system will fail. Let T_C represent the time when the system failure occurs, then the reliability of the system for time slot t is:

$$P_r(T_C \geq t) = P_r(Z(t) \leq C) \qquad (3)$$

3.2. EVA's V2G reliability model

A Poisson process can be used to describe the number of random occurrences or attendant arrivals of points in a given space. For example, the number of EVs arriving at the park position and staying there before time gap t can be considered as a Poisson process. To model the V2G reliability of the EVA, the following reasonable assumptions can be made:

(1) Each time slot EV participates in a Poisson process with parameter λ for the number $N(t)$.

(2) The amount of electricity that the ith EV can participate in V2G is V_i, and let $V_1, V_2, \ldots, V_n$ be independent of each other and identically distributed.

(3) The number of EVs participating in V2G in a time slot is independent of the amount of power available to them to participate in V2G.

Considering the EV arriving at the park position and staying before time slot t as an event, and the power that EVA can provide to the grid via V2G at time slot t as a random variable accompanying the event, the composite Poisson distribution can be applied to calculate the reliability of EVA's V2G at time slot t.

Let $V_0 = 0$, the probability of EVA completing the bidding value at time slot t is:

$$\begin{cases} P_r[Z_t > C] = P_r[\sum_{i=1}^{N_t} V_i > C] = \sum_{N_t=0}^{\infty} F_t^{(N_t)}(V_t) \frac{\lambda^{N_t}}{N_t!} e^{-\lambda} \\ 0 \leq N_t \leq n, (N_t \in N) \end{cases} \qquad (4)$$

In the formula, C is the bidding value of EVA; N_t is the number of EVs actually involved in the discharge activity in time slot t; V_i is the V2G discharge of the ith EV in the time slot; Z_t is the total amount of power available for the EV cluster to participate in V2G, when $Z_t < C$, denotes that the tth time slot EVA has not completed the bidding task. n is the number of EVs contracted with the aggregator; λ is the number of EVs involved in the discharge per unit time slot. $F_t^{N_t}(V_t)$ represents the distribution function of V_t within time slot t. Influenced by EV travel habits, with different time slots and different $F_t^{N_t}(V_t)$.

The expected value of the number of EVs participating in V2G at the beginning of each time slot is rounded to the Poisson parameter λ for that time slot:

$$\lambda = n - [\sum M_t p(M_t)], \lambda, t \in N \qquad (5)$$

In the formula, M_t is the total number of missed EVs in the tth time slot; $p(M_t)$ is the probability of occurrence of the corresponding default EV quantity value in the statistical time period.

In order to obtain the probability distribution of the Equation (4), it is necessary to first obtain the daily value of power that can participate in V2G for each contracted EV and the probability distribution of power that can participate in V2G for the EV group.

3.3. Estimated available V2G power for a single EV

The remaining power of the EV user battery is directly related to its available V2G power [25]. In this paper, the confidence interval for the average daily consumption of EV is estimated by approximating the normal distribution [23], and the average daily consumption of EV users at confidence level $1 - \beta$ is defined as:

$$H_{av} = \overline{C_{av}} \pm \frac{z_{\beta/2} s}{\sqrt{N}} \qquad (6)$$

In the formula, $\overline{C_{av}}$ is the average of the charging volume calculated by analysing the EV charging values throughout the year; $z_{\beta/2}$ is the value of the z statistic at the confidence interval; s is the standard deviation from the analysis of the annual charging values; N is the number of days included in the year.

Based on the previous content, it can be assumed that the EV is fully charged at the beginning of the day so that the maximum discharge can be achieved during the peak daytime load. And in order to prevent the battery over-discharge

damage to the battery, set the minimum State of Charge (SOC) to 0.2 after V2G discharge and driving.

Then the daily V2G power of EV user i is:

$$E_{i,start}^{V2G} = 80\%BE - H_{av} \qquad (7)$$

In the formula, BE is EV battery capacity.

At time slot t, EV user i's engageable V2G power is:

$$E_{i,t}^{V2G} = E_{i,start}^{V2G} - \sum Q_{i,t} \qquad (8)$$

In the formula, $\sum Q_{i,t}$ – is the amount of power that has been bid and allocated by EV before time slot t.

3.4. Probability distribution of EV clusters $F_t^{(N_t)}(V_t)$ that can participate in V2G power within time slot t

The amount of V2G discharge that an EV user can participate in at time slot t is also affected by whether that EV has already participated in V2G before time slot t.

Since EVs travel differently in different time slots, then there are some EV users who miss their appointment in the first time slot, resulting in less V2G discharge for the EV cluster in the first time slot; or users have already participated in V2G before the first time slot, resulting in less V2G power available for the EV cluster in the first time slot. Due to the strong fit of the Gaussian mixture distribution, the total available V2G power of the first time slot EV cluster still satisfies the Gaussian mixture distribution under these variation conditions, nevertheless with different distribution parameters.

The probability density function of the Gaussian mixture distribution is:

$$p(x|\theta) = \sum_{k=1}^{K} \beta_k \varphi(x|\theta_k) \qquad (9)$$

In the formula, $\beta_k \geq o$, this represents the value of the weighted coefficient of the k Gaussian components; $\varphi(x|\theta_k)$ is the probability density function of the kth Gaussian component.

The distribution function describing the discharge $\sum_{i=1}^{n} V_i$ of the EV group at the tth time slot using a Gaussian mixture distribution is as follows:

$$F_t^{(N_i)}(V_t) = \int_{\alpha}^{V_i} p(x|\theta)dx \qquad (10)$$

$$\varphi(x|\theta_k) = \frac{1}{\sigma_{k,t}} e^{-\frac{(x-\mu_{k,t})^2}{2\sigma_{k,t}^2}} \qquad (11)$$

$$\sum_{k=1}^{K} \beta_k = 1 \qquad (12)$$

In the formula, α is the minimum power supply of EVA in the tth time slot of EVA (in this paper, α is taken as the bidding value of EVA in the tth time slot); V_t is the maximum discharge of EVA in the EVA's tth time slot; $\sigma_{k,t}$, $\mu_{k,t}$ are the distribution parameter of the Gaussian mixture distribution; K is the order of the Gaussian mixture distribution model (K=1 or 2 in this paper). The time slots are different, the volume of EVs involved in V2G is different, and the distribution parameters are different.

Since the V2G power already released by the EV cluster to fulfill the contract before that time slot is considered at any time slot, some of the V2G power being released will change the subsequent discharge capacity of the EV cluster, thus affecting the distribution parameters of the hybrid Gaussian distribution. However, the Gaussian mixture distribution is obtained by weighting and summing multiple Gaussian components, and when calculating the parameters of each component, the analytical solution cannot be obtained directly by the derivative method due to the difficulty in deriving the likelihood function and the singularity of the distribution itself.

4. EV clusters and PV participation in microgrid voltage coordination optimization

In this paper, the research context is set in a light and storage smart residential area, and the response resources include conventional adjustable load, PV, and EV. It is assumed that the grid dispatching centre does not consider the EVA's ability to provide standby capacity when formulating the day-ahead operation plan, and gives priority to invoking local flexibility resources when a disturbance occurs during intra-day operation to ensure safe and stable operation of the microgrid. Based on this, this paper proposes an intra-day dispatching model for distribution networks, and simulates and analyses various possible disturbance scenarios by continuously optimizing the objective function through Genetic Algorithms.

With minimum voltage fluctuation, minimum network loss and minimum power fluctuation of the main-distribution network contact line as the objective function:

$$MinF = \varepsilon_1 \Delta U + \varepsilon_2 P_{loss} + \varepsilon_3 \Delta P_{line} \qquad (13)$$

ε is the weight coefficient of the elements of the objective function, which is assigned as follows: $\varepsilon_1 + \varepsilon_2 + \varepsilon_3 = 1$; $\varepsilon_1 = 0.3, \varepsilon_2 = 0.2, \varepsilon_3 = 0.5$.

The AC current constraint is as follows:

$$\begin{cases} P_{ij,t} = \sum_{n:j \to n} P_{jn,t} + r_{ij}(I_{ij,t})^2 + P_{j,t} \\ Q_{ij,t} = \sum_{n:j \to n} Q_{jn,t} + x_{ij}(I_{ij,t})^2 + Q_{j,t} \\ P_{j,t} = P_{d,j,t} - P_{EV,j,t} - P_{PV,j,t} \\ Q_{j,t} = Q_{d,j,t} - Q_{EV,j,t} - Q_{PV,j,t} \end{cases} \qquad (14)$$

In the formula, $P_{j,t}$, and $Q_{j,t}$ denote the net active and reactive power injected at node j at moment t; $P_{d,j,t}$, and $Q_{d,j,t}$ denote the active and reactive power of the load at node j at time t; $P_{EV,j,t}$, and $Q_{EV,j,t}$ denote the active and reactive power injected by EV at moment t and node j; $P_{PV,j,t}$, and $Q_{PV,j,t}$ denote the active and reactive power injected by PV at moment t and node j.
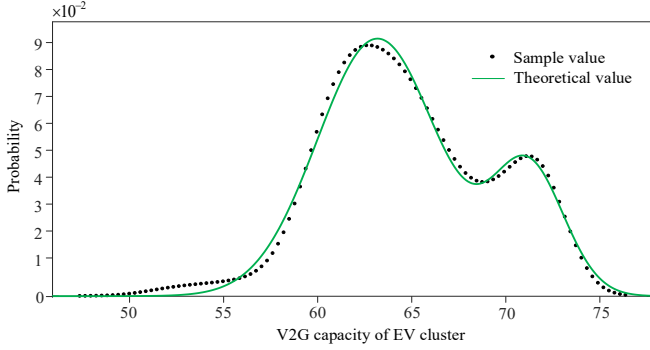
Safe operating constraints:

$$\begin{cases} V_{i.min} \leq V_{i,t} \leq V_{i.max} \\ I_{ij,t} \leq I_{ij.max} \end{cases} \qquad (15)$$

In the formula, $I_{ij,max}$ is the upper limit of the current amplitude transmitted by the branch ij.

Microgrid and main grid contact line power constraints:
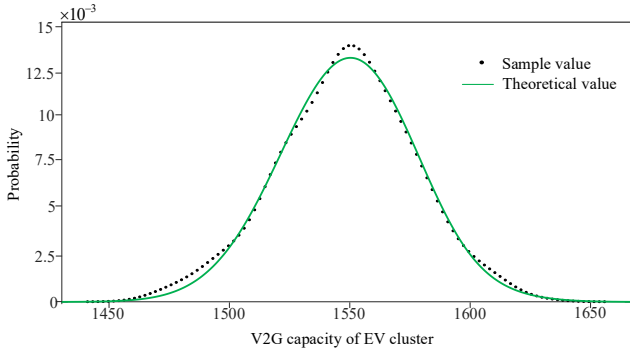
a) Day Initial Time Slot All EV Participation V2G Situation

b) Arbitrary selection of some EVs to participate in V2G situations

Figure 3 *Sample distribution and theoretical distribution of EV cluster's V2G capacity*

Table 1 Quantitative basis for EV user classification

Type of users	Habitual charge periods	Desired charge value $\overline{Q_d}$/kWh	Desired charge interval *In(h)*
Short commute users	Non-work time	$3 < \overline{Q_d} \leq 6$	$12 < In \leq 45$
Long commute users	Non-work time	$\overline{Q_d} > 6$	$0 < In \leq 12$
Residential users	Free time	$\overline{Q_d} \leq 3$	$In > 45$

Table 2 Data distribution of various types of EV users

Type of users	Desired average power loss H_{av}/kWh	Available V2G capacity $E_{i,\,start}^{V2G}$/kWh
Short commute users	[4.456,5.353]	[17.819,18.782]
Residential users	[1.720,2.274]	[24.811,25.366]
Long commute users	[8.970,10.363]	[17.541,18.934]

$$P_{grid}^{min} \leq P_{grid} \leq P_{grid}^{max} \qquad (16)$$

In the formula, $P_{grid}^{min}, and\ P_{grid}^{max}$ are the upper and lower limits of contact line power respectively.

The active and reactive power output constraints of PV:

$$\begin{cases} P_{PV,j} = P_{PV,j,MPPT} \\ (P_{PV,j,t})^2 + (Q_{PV,j,t})^2 \leq (S_{PV,j})^2 \end{cases} \qquad (17)$$

In the formula, $P_{PV,j,MPPT}$ is the active power injected when the PV at node j is operating at the *MPPT* point; $S_{PV,j}$ is the installed PV capacity of node j.

EV condition constraints:

$$\begin{cases} P_{EV,j,min} \leq P_{EV,j,t} \leq P_{EV,j,max} \\ (P_{EV,j,t})^2 + (Q_{EV,j,t})^2 \leq (S_{EV,j,max})^2 \\ E_{EV,j,t+1} = E_{EV,j,t} - \frac{P_{EV,j,t}\Delta t}{\eta_{Dis,j}}, P_{EV,j,t} \leq 0 \\ E_{EV,j}^{max} \times 20\% \leq E_{EV,j,t} \leq E_{EV,j}^{max} \times 80\% \\ P_{rel} \geq 0.95 \\ E_{rel}^{V2G} \geq E_{fore}^{V2G} \end{cases} \qquad (18)$$

In the formula, $S_{EV,j,max}$ denotes the maximum apparent power of node j energy storage inverter; $P_{EV,j,t}$ is the discharge power of EV at moment t; $E_{EV,j,t}$ and $E_{EV,j}^{max}$ denote the storage capacity and maximum storage capacity of the electric vehicle at node j at moment t; $\eta_{Dis,j}$ indicates EV discharge efficiency; P_{rel} is the reliability of the contracted V2G power available from EVA at a certain moment; E_{rel}^{V2G} is the actual V2G capacity that EVA can provide; E_{fore}^{V2G} is the capacity of the EVA day-ahead forecast.

5. Simulation analysis of EV reliability

5.1. EV historical charging data introduction

The analysis of 74 EV customers from Pecan Street Inc.'s 2015 annual electricity consumption dataset [21] is used to verify the validity of the V2G reliability model proposed in this paper for EVA and to analyse the factors affecting the reliability of EVA's participation in V2G. The dataset contains customer electricity consumption data from the states of Texas, Colorado and California with data resolution of 1 minute.

In this paper, with reference to the working hours of the data set collection area and the footprint of the area, we set the working hours of commuting users from 9:00 am to 5:00 pm. Assuming that every 15 min is a time slot, a day contains 96 time slots. By analysing historical charging data, users can be classified as short commute users, long commute users, and residential users. The classification criteria are shown in Table 1, containing 41 short commute users, 25 long commuter users, 8 residential users. The data characteristics of typical EV users are shown in Table 1.

According to the method proposed in Section 3.3 of this paper, the expected interval of daily power consumption for each type of EV users and the daily interval values of V2G power that can be participated are obtained, as shown in Table 2.

5.2. Probability distribution of t-time slot EV clusters that can participate in V2G power

Figure 3(a) gives the sample distribution of the EVA available V2G power obtained for the initial time slot of the day, with all 74 EV users participating in V2G, compared with the theoretical Gaussian mixture distribution. Some EVs were randomly selected to participate in V2G to simulate the situation where any t time slot in the day is not available for

Table 3 Gaussian mixture distribution parameters for different scenarios

Number of users	$\sigma_{1,t}$	$\mu_{1,t}$	$\sigma_{2,t}$	$\mu_{2,t}$	β_1	β_2
74	29.196	1551	17.579	1593	1.001	0
3	3.202	63.18	1.907	71.19	0.768	0.232

Table 4 Participate in V2G power probability distribution goodness of fit

Number of users	Figure	SSE	SST	R-square
74	Fig 3(a)	0.000094	0.004	0.9965
3	Fig 3(b)	0.00066	0.10030	0.9934

Table 5 Variation trend of EVA reliability in different time slots with bidding value

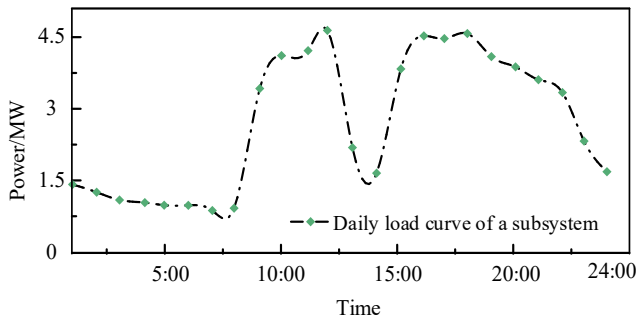| EVA bidding value W_t^{max} /kWh	EVA reliability of different time slots		
	10:31～10:45	13:31～13:45	18:01～18:15
950	0.9935	0.9729	0.9426
1000	0.9859	0.9492	0.9015
1050	0.9674	0.9001	0.8232
1100	0.9411	0.8405	0.7399
1200	0.8783	0.7226	0.5915
1300	0.7617	0.5533	0.4104
1400	0.6509	0.4223	0.2878

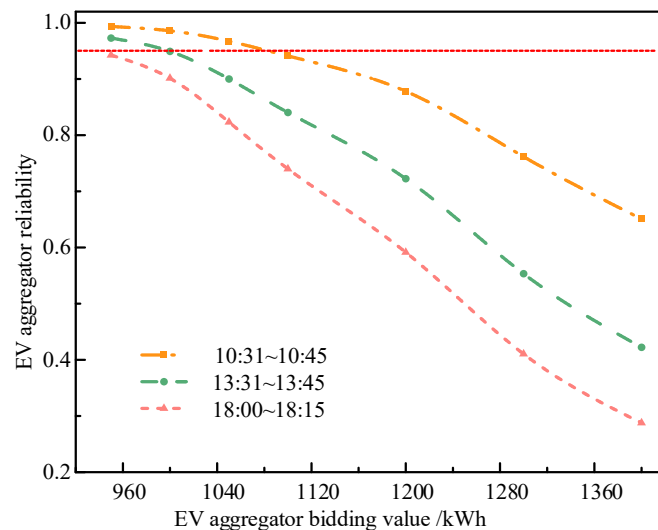***Figure 4*** *Intraday load curve of a subsystem*

Figure 5 *Variation trend of EVA reliability in different time slots with bidding value*

performance due to some EVs. Figure 3(b) shows the sample and theoretical distributions of V2G power for EVA in this case.

The parameters of the Gaussian mixture distribution obtained by fitting the two cases of Figure 3 are given in Table 3.

The results of the Gaussian mixture distribution goodness-of-fit tests for both cases are given in Table 4. The fit was evaluated based on the sum of squares due to error (SSE), total sum of squares (SST), and coefficient of determination (R-square). The closer the R-square is to 1, the better the model is able to explain the sample data. From the evaluation results, it is clear that the probability distribution of EVAs that can participate in V2G power can be described by a Gaussian mixture distribution with different parameters, whether all EVs or some EVs participate in V2G, in scenarios where the number of EVs participating and the amount of power vary.

5.3. Reliability analysis of EVA participation in V2G

This subsection discusses the reliability of EVA participation in V2G and its influencing factors in two cases: 1) EV users participate in V2G only once per day; 2) EV users can participate in V2G multiple times per day.

Figure 4 shows the intra-day load curve of a subsystem [26], with a time slot of 15 min. From Figure 4, the lunch peak hour is (10:00 to 13:30) and the evening peak hour is (18:00 to 21:00). It is assumed that EVA bids for spare capacity during the peak hours.

5.3.1 Analysis of EVA for bidding value and reliability: This section calculates the bidding value and its reliability of V2G participating in day $t+1$ by extracting day t from the historical data, using the charging data before day t as the historical data, and combining it with the model in this paper. And the actual travel data of EVs on day $t+1$ are used to verify the calculation results.

1) EV users participate in V2G once a day

In this paper, three time slots of a certain day are randomly selected for analysis, and the trend of EVA reliability with bidding value for different time slots is given in Table 5.

The variation curves of EVA reliability with the bidding value at different time slots are shown in Figure 5.

As can be seen in Figure 5, the amount of bidding value for EVA to achieve the same reliability varies at different time slots during the day, depending on customer travel. Table 6 gives the available V2G power for the EV cluster based on the actual trips made by EV users on the second day in the above three time slots.

Table 6 shows the calculated bidding value and their reliability obtained on day t verified with the actual V2G power of the corresponding time slots on day $t+1$. It can be seen that the V2G power for each time slot on day $t+1$ can achieve a reliability of 0.9 or more, and their V2G power are all greater than the lowest V2G power when the reliability is 0.95. Therefore, the method proposed in this paper can be effectively used to guide the selection of EVA bidding value for a certain time slot.

Table 6 EV clusters can participate in V2G electricity in corresponding time slots on the next day

Types	Time slot	10:31～10:45	13:31～13:45	18:01～18:15
t+1 available capacity V2G /kWh		1183.75	1052.33	1000.36
Reliable power interval		≥1090	≥ 1000	≥950

Table 7 Comparison of EVA reliability under two allocation schemes of different time slots

First time slot (10: 00～10: 15]			Second time slot (18: 30～18: 45]		
EVA bidding value /kWh	Priority reliability	Average reliability	EVA bidding value /kWh	Priority reliability	Average reliability
475	0.9793	0.8651	450	0.9761	0.9160
500	0.9600	0.8558	500	0.9456	0.8830
550	0.8669	0.7857	535	0.9030	0.8098
600	0.7605	0.6282	550	0.8761	0.7822
650	0.5994	0.3958	600	0.7287	0.5876
700	0.4693	0.1628	650	0.5532	0.3405

2) Daily participation in multiple V2G situations

EVA may bid for multiple time slots and also allow EVs to participate in V2G at multiple time slots, in which case it is necessary to consider how each bidding value of EVA is distributed among multiple EV users. There are two possible allocation schemes.

a) Priority distribution

EV users are ranked from highest to lowest priority, and those with higher priority are given priority to participate in V2G. In this paper, the priority of the EV is determined by the SOC value of the EV at the arrival of time slot *t*. The higher the charge state is, the higher the priority is. End the assignment task when equation (12) is satisfied.

$$C_t \leq \sum_{i=1}^m E_{i,start}^{V2G} \tag{19}$$

In the formula, C_t is the EVA bid for the *t*th time slot; m is the number of EV participants that satisfy the bidding value at time slot *t*.

It is assumed that EVs that obtain discharge eligibility release all of their V2G-capable capacity. At the arrival of the next time slot, the EVA updates the EV charge status, re-issues the discharge priority, and participates discharge task in the next time slot.

b) Average distribution

EVA distributes the bidding value equally to all contracted EV customers based on the bidding value at time slot *t*. Take the example of EVA bidding on two different time slots for the following day. The two bidding time slots chosen are (10:00~10:15] and (18:30~18:45]. The variation of EVA reliability with the bidding values for the two different allocation schemes is shown in Table 7.
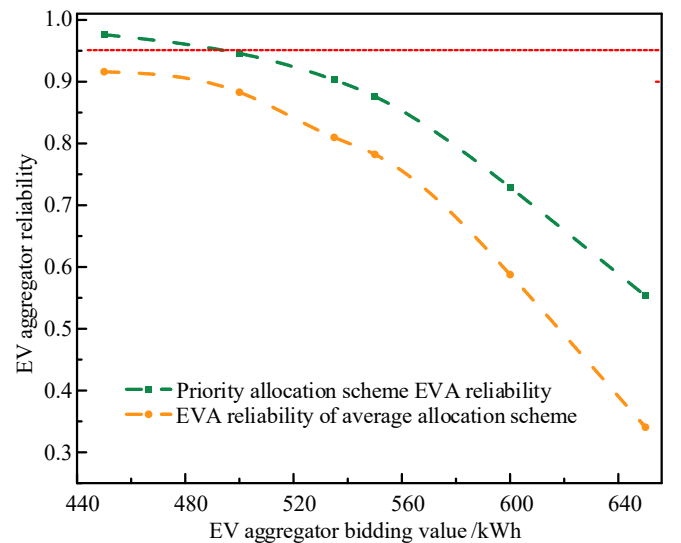
The EVA reliability variation curves for different time slots are shown in Figure 6. The priority allocation scheme has higher reliability compared to the average allocation scheme for the same bidding value. For the same reliability constraint, the bidding value of EVA in the priority allocation

scheme is able to reach a larger value. When EVA bidding value is specified, a single EV in the priority allocation scheme has a higher allocated power in each time slot, which can more fully exploit the discharge potential of EVs. When EVAs give the same unit price of economic incentives to EVs, EV users in the priority allocation scheme have higher benefits. The priority allocation scheme is better than the average allocation scheme from both the reliability point of view and the economic point of view.

5.3.2 Impact of different types of EV user share on EVA reliability: Residential users travel less frequently, so their randomness is low and they are less likely to miss appointments. Long-range commuters with higher daily power consumption and longer driving distances are less likely to park their cars than residential users and short commuter users, and their likelihood of missing appointments is higher. In this section, different numbers of the three types of users are selected, and four ratio cases are constructed
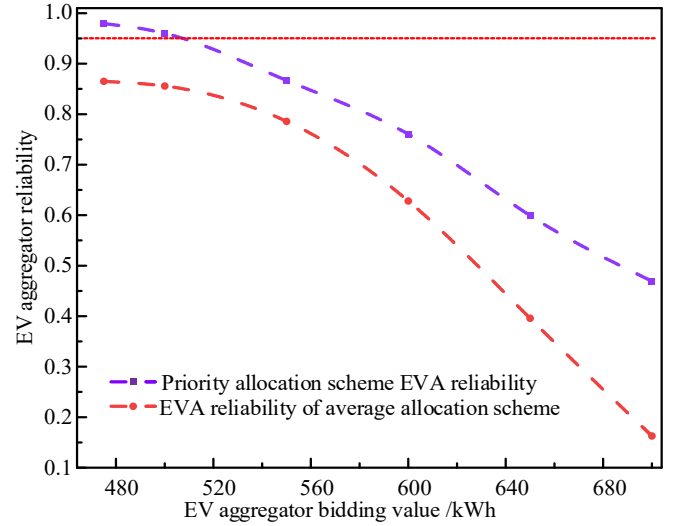
a) EVA reliability curves under two allocation schemes for time slot 1

b) EVA reliability curves under two allocation schemes for time slot 2
Figure 6 EVA reliability curves of two allocation schemes at different times

Table 8 Poisson parameters for different proportions of users

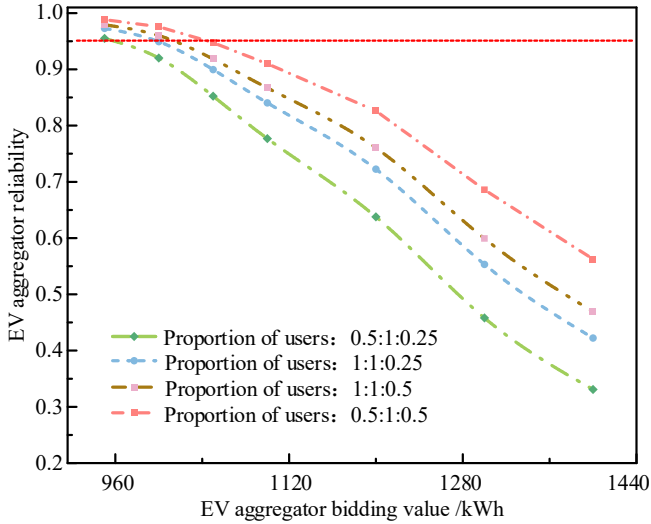| Proportion of different types of users	Poisson distribution λ
1.5：1：0.25	66
1：1：0.25	68
1：1：0.5	69
0.5：1：0.5	71

Figure 7 *EVA reliability curve under different EV type proportions*

according to the ratio of the number of long commute users and short commute users: the number of residential users as 1.5:1:0.25, 1:1:0.25, 1:1:0.5 and 0.5:1:0.5. The Poisson parameters at different user ratios are shown in Table 8.

The V2G reliability variation curves of EVAs under different EV type share scenarios are shown in Figure 7.

As can be seen from Figure 4, the higher the percentage of residential users and the lower the percentage of long commute users, the higher the reliability of EVAs, and the higher the amount of electricity bid by EVAs subject to the same reliability constraints to participate in V2G. Therefore, EVA should selectively contract EV customers that can increase their V2G bids for power at different time slots while meeting reliability constraints.

6. Simulation analysis of microgrid voltage optimization

In the new electricity power system, the power output of new energy sources such as PV is unstable, and the actual power output deviates from the predicted power output, which may affect the safe and stable operation of voltage. EV can be used as distributed energy storage for optimal scheduling. In this paper, we use Genetic Algorithm to simulate various scenarios of EVA and PV coordinated optimization of microgrid voltage based on the improved IEEE 33 node system. Comparison of simulation results to verify the effect of different EVA "bidding value-reliability" on voltage optimization of microgrid at different times. Finally, the economics of the microgrid and the economics of EVA are discussed. This section assumes that the Point of Common Coupling (PCC) is disconnected and the microgrid is in islanded operation when a disturbance occurs in the microgrid.

6.1. Forecasted power purchases from the microgrid to the main grid under normal operation

In the modified IEEE 33 node system, nodes 4, 6, 7, 11, 16, 21, 24, 29 are added to the PV (shown in Figure 8), and the PV output parameters are shown in Table 9. The IEEE 33 node has an active power of 3715 kW, a reactive load of 2300 kvar, and a voltage reference of 12.66 kV [27]. The genetic optimization algorithm selects the population size M=40, the crossover probability Pc is 0.8, and the variation probability Pm is 0.1, the algorithm diagram is shown in Figure 9. The whole simulation process was carried out in MATLAB 2020a with a computer processor Intel(R) Core(TM) i5-8250U running at 1.8GHz CPU and 8.00GB RAM.

The power purchased by the microgrid from the main grid at each moment during the day is:

$$E_{mic}(t) = P_{load}(t) - P_{pv}(t) \qquad (20)$$

In the formula, $P_{load}(t)$ is the predicted value of load at time t; $P_{pv}(t)$ is the PV forecast generation at time t.
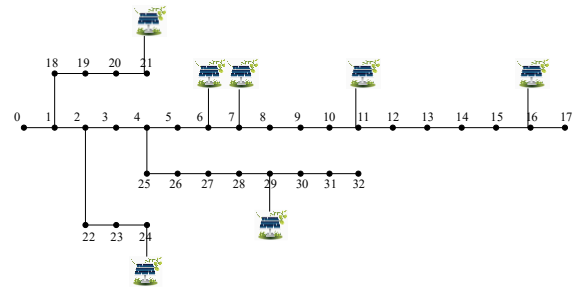

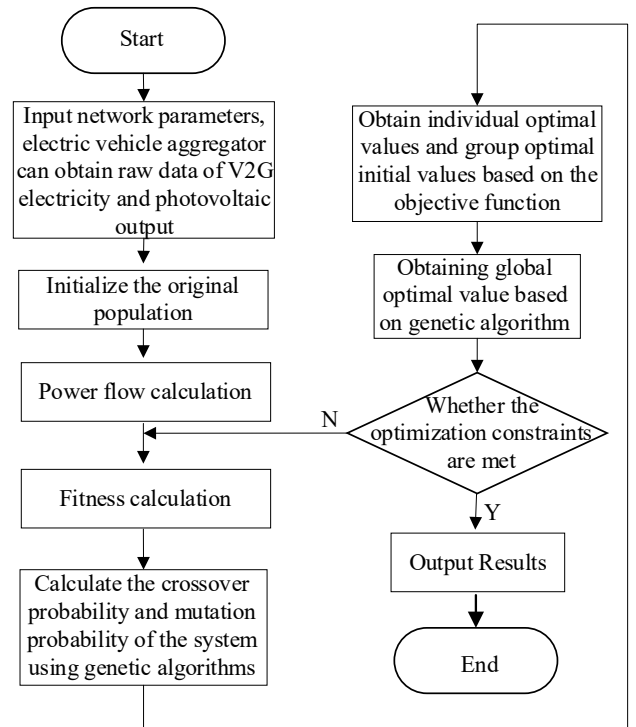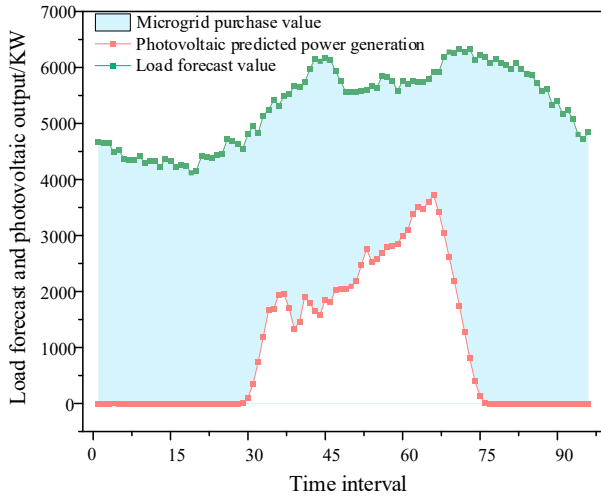***Figure 8*** *IEEE 33 node topology with PV during normal operation*

Figure 9 *Genetic Algorithm flow*

Table 9 Photovoltaic output data parameters

PVs number	System node number	Rated capacity /kVA	Actual merit contribution/kW
1, 3, 5, 7	4, 7, 16, 24	800	650
2, 4, 6, 8	6, 11, 21, 29	600	450

***Figure 10** Load forecast value, PV output value and microgrid power purchase graph*

In this paper, the load forecast data and PV output forecast data of a park in Nanjing are selected to predict and calculate the power purchase of microgrid during normal operation, and the calculation results are shown in Figure 10. The load forecast value, PV output value and power purchase of microgrid are shown in Table A1.

As mentioned earlier, the coordination potential of distributed energy storage in the microgrid is not mobilized during normal operation. In order to ensure the safe and stable operation of the microgrid, the distributed energy storage represented by EVA is responsible for coordinating and optimizing the operation of the microgrid when the demand-side power of the microgrid is in shortage due to factors such as excessive forecast errors of PV output or excessive load fluctuations.

6.2. Voltage optimization of microgrid considering the prediction error of PV power generation

The bidding value and the reliability are inversely proportional to each other at a certain point in time because the maximum V2G power available from EVA is fixed. When there is a serious deviation in the forecast of PV output in the micro-grid system, resulting in less power generation than the generation plan, if the EVA does not have the reliability as a reference before bidding and bids blindly, the bidding value is less than the maximum V2G power that EVA can provide at this moment, it can achieve the purpose of filling the power shortage, and vice versa, it will lead to a certain shortage of load in the system, making the micro-grid voltage and network loss fluctuate too much. To be conservative, this section assumes that the grid dispatch centre only allows EVA to release V2G power with reliability of 0.95 and above, which will be defined as reliable power. When the EVA bidding value exceeds the reliable power it can provide at the corresponding moment, the default EVA will be released according to the reliable power; when the EVA bidding value

is lower than the reliable power it can provide, it will be released strictly according to the bidding value. In this section, on the basis of section 6.1, EV clusters are successively added to the end nodes of lines such as nodes 14 and 30 to optimize the microgrid voltage in coordination with PV, and the upper and lower limits of voltage deviation are set from 0.95pu to 1.02pu.

The table 10 as follows shows the in-system power deficit corresponding to EVA reliability, using the second time period of Table 5 as an example.

Taking the time period of 13:31-13:45 as an example, the maximum V2G power available from EVA is 985kwh in this time period under the premise of reliability. Figure 11 and Figure 12 shows the curves of node voltage optimization effect with EVA "bidding value-reliability" at different moments of deviation of PV output forecast in the microgrid system and different EVA access node scenarios.

Table 10 Correspondence between EVA reliability and PV outage power supply

Times	EVA bidding value/kWh	reliability	Power shortage /kWh	PV forecast deviation	Reliable power /kWh
13:31-13:45	950	0.9729	950	21.5%	950
	985	0.9502	985	22.4%	985
	1000	0.9492	1000	22.7%	985
	1050	0.9001	1050	23.9%	985
	1100	0.8405	1100	25%	985
	1200	0.7226	1200	27.3%	985
	1300	0.5533	1300	29.5%	985
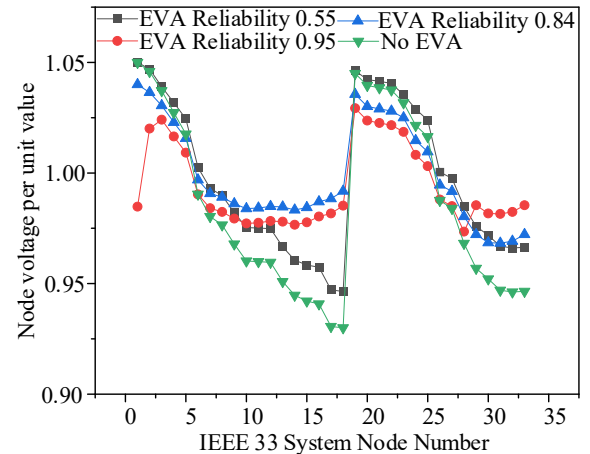
***Figure 11** EVA is located at node 30, node voltage optimization with EVA reliability variation curve*
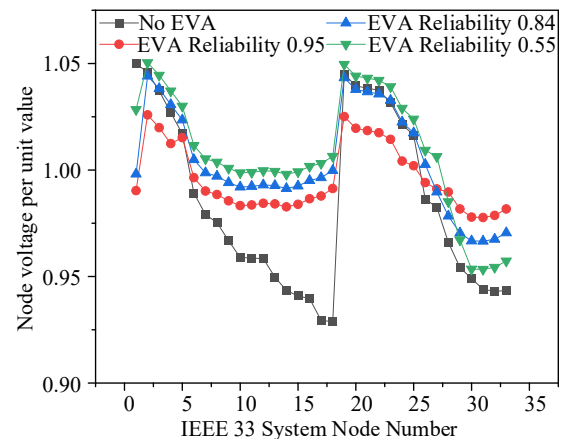
***Figure 12** EVA is located at node 14, node voltage optimization with EVA reliability variation curve*
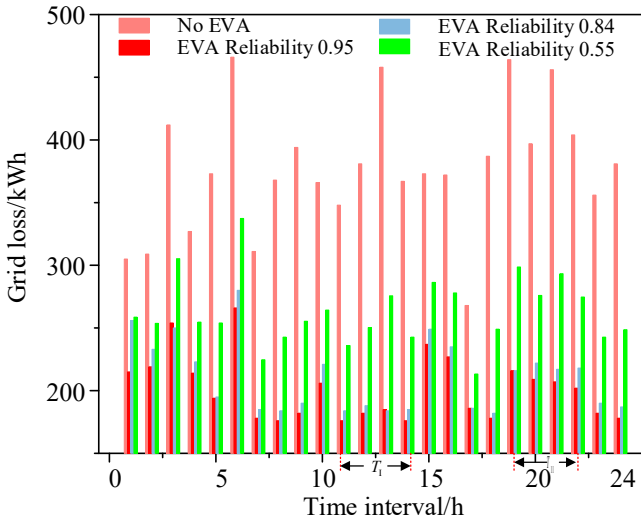
Figure 13 *System network loss fluctuation curves under different EVA reliability when PV prediction error is too large*

It is obvious from Figures 10 and 11 that the voltage fluctuation range is smoother when EVA is involved in the coordinated optimization of microgrid voltage. When EVA is involved in different reliability degrees, the higher its reliability degree, the more obvious the voltage optimization effect is and the smoother the fluctuation is. Only when the reliability degree is 0.95, the voltage optimization result is between the set 0.95pu and 1.02pu.

Under the same scenario of PV power output prediction error, this section shows the relationship between network loss and contact line power fluctuation within the system and EVA reliability in two peak load hours of 10:30-14:30 and 19:00-22:00 with node 30 injecting EVA available V2G power as an example, as shown in Figure 13.

When the EVA is not involved in V2G behaviour, the fluctuation of network loss during peak load hours is large, and when the EV is injected into the microgrid with different reliability levels, it is obvious that the fluctuation of system network loss is significantly reduced. When the EVA reliability is 0.95, the expected value of network loss in time period T_1 is reduced from 382.17kWh to 193.67kWh, and the expected value of network loss in time period T_2 is reduced from 426kWh to 202.5kW. Among them, the higher the reliability of EVA, the smoother the fluctuation of network loss.

6.3. Voltage optimization of microgrid considering distribution network load fluctuations

Grid dispatching is divided into two types: day-ahead dispatching and real-time dispatching, and in general, real-time operation is not exactly the same as day-ahead plan making. Real-time fluctuations in distribution network load are the root cause of load peaks or load dips. During low load hours, thermal units can meet load fluctuations with a small rotating reserve, but during peak load hours, especially when fluctuations are too large, PV output is not sufficient to meet load shortages, and due to safety constraints, thermal units cannot increase rotating reserve output to a large extent. In this section, under the scenario of large fluctuations in distribution network load and small errors in PV output

prediction, the EVA participates in V2G discharge to reduce or avoid interrupting or shifting customer load and improve the customer's electricity experience.

This section takes the 3rd time period of Table 5 as an example. On the basis of section 6.1, EVAs are successively arranged at nodes 16 and 23 of the system to simulate and observe the impact of EVA reliability on the microgrid voltage, network loss and power fluctuation of the main distribution network contact line when the load fluctuates excessively. Table 11 presents data on the range of system load fluctuations corresponding to different reliability levels of EVA.

Figures 14 and 15 show the system node voltage optimization curves when the EVA is at nodes 14 and 23, respectively, when the load fluctuates excessively.

Table 11 Correspondence between EVA reliability and system load fluctuation

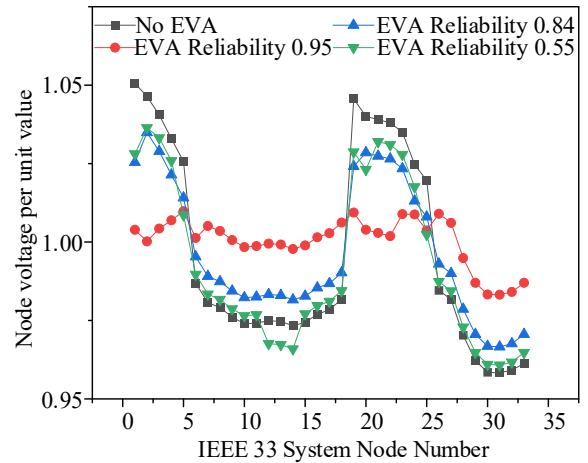| Time period	EVA bidding value /kWh	Reliability	Load fluctuation power /kWh	Reliabale power /kWh
18:01-18:15	935	0.9527	+935	935
	950	0.9426	+950	935
	1000	0.9015	+1000	935
	1050	0.8232	+1050	935
	1100	0.7399	+1100	935
	1200	0.5915	+1200	935
	1300	0.4140	+1300	935

Figure 14 *EVA is located at node 14, node voltage optimization with EVA reliability variation curve*
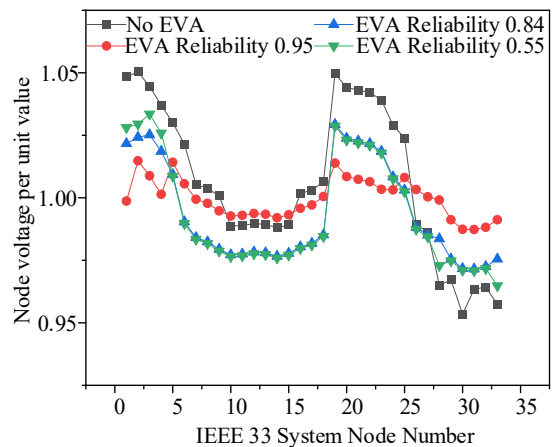

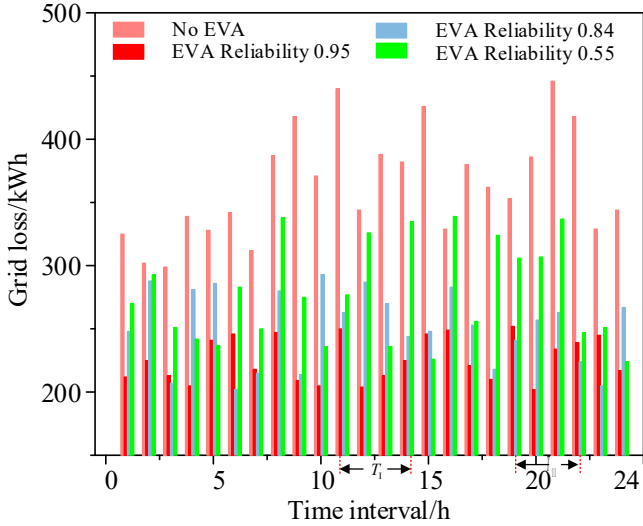**Figure 15** *EVA is located at node 23, node voltage optimization with EVA reliability variation curve*

10

Figure 16 *System network loss fluctuation curves under different EVA reliability when the load fluctuates too much*

Table 12 Customer time-of-use tariff

	Peak hours t_1	Normal hours t_2	Low hours t_3
Time period	10:00-14:00 18:00-22:00	6:00-9:00 15:00-17:00	0:00-6:00 22:00-24:00
Price/($/kWh)	0.28	0.12	0.061

Table 13 Reward and penalty unit prices for purchasing electricity from microgrid.

Power purchaser	Grid price	PV incentive price	PV penalty price	EVA incentive price	EVA penalty price
Microgrid price/$/kWh	0.068	0.032	0.140	0.360	0.380

Table 14 Microgrid economy comprehensive income

EVA scenario	users revenue ($)	Grid loss ($)	Grid cost ($)	PV cost ($)	EVA cost ($)	PV penalty cost ($)	EVA penalty cost ($)	Combined gains ($)
Non-EV	1231.60	78.53	184.29	122.68	0	0	0	846.11
P_r=0.95	1231.60	41.33	184.29	122.68	358.12	140.36	0	665.62
P_r=0.84	1231.60	48.09	184.29	122.68	399.85	156.74	43.89	677.33
P_r=0.55	1231.60	53.16	184.29	122.68	472.56	185.24	120.23	704.39

From Figure 14 and Figure 15, it is obvious that the voltage fluctuation of the microgrid is significantly reduced and the node voltage minimum value is between 0.95 and 1.02 when EVA is involved in voltage optimization. In addition, the higher the reliability of EVA, the smoother the voltage fluctuation of the microgrid, so it can be seen that EVA is necessary to bid according to the reliability before the day.

In the same scenario of distribution network load fluctuation, this section shows the relationship between network loss fluctuation and EVA reliability within the system in two peak load hours of 10:30-14:30 and 19:00-22:00 with node 23 injecting EVA available V2G power as an example, as shown in Figure 16.

When the EVA is not involved in V2G behaviour, the network loss fluctuates significantly during peak load hours T_1 and T_2. When the EV is injected into the microgrid with different reliability levels, it is obvious that the system network loss fluctuation is significantly reduced. However, when the EVA reliability is 0.55, although the network loss decreases, the fluctuation is larger than the scenario when the reliability is high. When the EVA reliability is 0.95, the expected value of network loss in time period T_1 is reduced

from 382.17kWh to 193.67kWh, and the expected value of network loss in time period T_2 is reduced from 426kWh to 202.5kWh. When the distribution network load fluctuates too much, the higher the EVA reliability, the smaller the network loss and the smoother the fluctuation.

6.4. Exploring microgrid economics and EVA economics

To optimize the system operation, in addition to considering the system operation safety, reliability and flexibility, the economy should also be considered. This section describes the micro-grid and EVA economic calculation methods, and discusses the micro-grid economy and EVA economy respectively.

6.4.1 Exploring the economics of microgrids: In the microgrid system described in this paper, the scope of power purchase for the microgrid is the main grid, PV, and EVA, and the load hours are divided into three categories: peak hours, usual hours, and low hours[28]. The unit price of electricity for customers in each time period is shown in Table 12.

At moment t, the purchased power cost of the microgrid is calculated as follows:

$$C_{mic}(t) = C_{maj,t}P_{maj}(t) + C_{pv,t}P_{pv}(t) + C_{eva,t}P_{eva}(t) \quad (21)$$

In the formula, $C_{maj,t}$, $C_{pv,t}$, and $C_{eva,t}$ are the unit prices of electricity purchased by the microgrid from the main grid, PV, and EVA at time t; $P_{maj}(t)$, $P_{pv}(t)$, and $P_{eva}(t)$ are the values of electricity purchased by the microgrid from the main grid, PV, and EVA at moment t.

The economic gain of the micro network at moment t is:

$$In_{mic}(t) = C_{load,t}P_{load}(t) - C_{load,t}P_{loss}(t) - C_{mic,t} + \beta_{eva}P'_{eva} + \beta_{pv}P'_{pv} \quad (22)$$

$$C_{load,t} = \begin{cases} C_{load}^1 & t \in t_1 \\ C_{load}^2 & t \in t_2 \\ C_{load}^3 & t \in t_3 \end{cases} \quad (23)$$

In the formula, $C_{load,t}$ is the unit price of electricity used by the load at time t; $P_{load}(t)$ and $P_{loss}(t)$ are the value of load and network loss at time t; C_{load}^1, C_{load}^2, and C_{load}^3 are the unit prices of electricity consumption in peak hours, normal hours and low hours; β_{eva} is the penalty unit price when EVA does not satisfy the reliability; β_{pv} is the penalty unit price when PV has forecast error; P'_{eva} is the difference between the EVA bidding value and the actual discharge; P'_{pv} is the error power predicted by PV.

When EVA does not meet the reliability, the penalty price for PV is 0.380$/kwh[23] and the penalty price for PV is 0.140$/kWh[29-31]. The unit prices of power purchases from the microgrid to the main grid, PV, and EVA are shown in Table 13.

The cost of the microgrid with different levels of EVA participation was calculated and compared using the EVA reliability at the moment of 13:31-13:45 as a reference. The results of the microgrid economic benefits calculation are shown in Tables 14.

Table 15 EVA economic benefits analysis

EVA reliability	EVA gains （$）	Grid penalty cost （$）	Pay for EV （$）	Combined gains （$）
P_r =0.95	358.05	0.00	288.45	69.61
P_r =0.84	399.85	43.89	288.45	67.52
P_r =0.55	472.56	120.23	288.45	63.88

From table 14, it can be seen that the microgrid revenue in the microgrid with EVA participation is lower than the revenue without EVA participation, which is due to the higher unit price of V2G tariff considering the battery depreciation cost as well as charging cost of the user. The lower the EVA reliability, the higher the microgrid revenue, but it seriously affects the day-ahead scheduling plan and damages the microgrid voltage stability.

6.4.2 Exploring the economics of EV aggregators: EV aggregator economic return is the price after removing the penalty charge of the micro network to the EVA and the V2G cost paid to the EV users. The equation is as follows:

$$In_{eva}(t) = C_{eva,t}P_{eva}(t) - \beta_{eva}P'_{eva} - C_{ev,t}P_{ev} \quad (24)$$

In the formula, $C_{ev,t}$ is the V2G unit price of EV discharged at the aggregator at time t; P_{ev} is the actual value of V2G power released by the EV cluster at moment t; The unit price for EV participation in V2G is set at 0.293 $/kWh[23]. The economic benefits of EV aggregators under different EVA reliability scenarios were calculated and compared, and the results are shown in Table 15.

From the calculation analysis, it can be seen that the EVA has different benefits when the reliability is different, and the higher the reliability, the higher the benefits. This is due to the fact that at a certain point in time EVA releases a certain amount of reliable power, and as the bidding value increases, the reliability decreases and the risk of penalties it receives rises accordingly, leading to a reduction in the final combined return.

7. Conclusion

In this paper, based on the characteristic that EV clusters can be used as distributed energy storage and considering their flexibility to participate in standby services, a reliability modeling method for EVA participation in V2G based on compound Poisson distribution considering the travel habits of contracted EV users is proposed, and EVA and PV are co-located in the microgrid for coordinated optimization of microgrid voltage. The following conclusions are obtained from the analysis of the above-mentioned paper:

(1) The distribution of V2G capacity and of any combination of EV user groups can be described by a mixed Gaussian distribution.

(2) Due to the stochastic nature of user travel behavior, the V2G power bid before the EVA day subject to the same reliability level is influenced by the moment of delivery.

(4) EVA reliability is influenced by the proportion of different types of EV users, and reasonable adjustment of the contracted proportion of each type of EV users can help EVA improve its own V2G reliability.

(5) In the micro-network structure in the paper, the higher the reliability of EVA can V2G power, the smaller the system voltage fluctuation and the lower the network loss. Its microgrid economics, although constrained by various energy prices, the higher the reliability of EVA in systems containing EVA, the better the microgrid economics. Since EVA is affected by default penalties, its economy likewise decreases as EVA reliability decreases.

8. References

8.1. Journal articles

[1] WANG M S, MU Y F, JIA H J, et al. A preventive control strategy for static voltage stability based on an efficient power plant model of electric vehicles [J]. Journal of Modern Power Systems and Clean Energy,2015,3(1)

[2] DEILAMI S, MASOUM A S, MOSES P S, et al. Real-time coordination of plug-in electric vehicle charging in smart grids to minimize power losses and improve voltage profile [J]. IEEE Transactions on Smart Grid, 2011, 2(3): 456-467

[3] WANG J J, JIA Y L, MI Z Q, et al. Reserve Service Strategy of Electric Vehicles Based on Double-incentive Mechanism [J]. Automation of Electric Power Systems,2020,44(10):68-76

[4] LUKAS D, LUIZ C P J, RICARDO R. Photovoltaics (PV) and electric vehicle-to-grid (V2G) strategies for peak demand reduction in urban regions in Brazil in a smart grid environment [J]. Renewable Energy,2014,68

[5] O'NEILL D, YILDIZ B, BILBAO J I. An assessment of electric vehicles and vehicle to grid operations for residential microgrids [J]. Energy Reports,2022,8

[6]LIU X F, ZHANG Q F, CUI S M. Overview of V2G technology for electric vehicles [J]. Transactions of China electrotechnical society, 2012, 27(2): 121-127

[7]WEN A L, HU Z C, NING J, et al. Bidding strategy for charging operators participating in peak shaving market based on distributed robust opportunity constrains [J]. Automation of electric power systems, 2022, 46(7): 23-32

[8]ZHANG J J, ZHANG P, WU H B, et al. Reliability and risk analysis of load aggregators in demand response [J]. Acta energiae solaris sinica, 2019, 40(12):3526-3533

[9] TING Z H, YUZE M, YUNNA W, et al. Optimization configuration and application value assessment modeling of hybrid energy storage in the new power system with multi-flexible resources coupling,Journal of Energy Storage,Volume 62,2023,106876,ISSN 2352-152X.

[10] HE J Q, SONG Z J, LAN Z, et al. Distribution Network Voltage Optimization Control Method Based on Model Predictive Control[P]. Information Technologies and Electrical Engineering,2019.

[11] TANG Z, HILL D J, LIU T. Fast distributed reactive power control for voltage regulation in distribution networks [J]. IEEE Transactions on Power Systems, 2019, 34(1): 802-805.

[12] KREIN P T, GALTIERI J A. Active management of photovoltaic system variability with power electronics [J]. IEEE Journal of Emerging and Selected Topics in Power Electronics, 2021, 9(6): 6507-6523

[14] LIU Y B, WU W C, ZHANG B M, et al. Active distribution network overvoltage prevention and control method based on active-reactive power coordination optimization [J]. Automation of electric power systems, 2014, 38(9): 184-191

[15] ZHICHUN Y, FAN Y, HUAIDONG M, et al. Review on optimal planning of new power systems with distributed generations and electric vehicles, Energy Reports, Volume 9, 2023, Pages 501-509, ISSN 2352-4847

[16] LI T, TAO S, HE K, et al. "Multi-objective Optimal Dispatching of Electric Vehicle Cluster Considering User Demand Response," 2021 IEEE 4th International Conference on Electronics Technology (ICET), Chengdu, China, 2021, pp. 1003-1008

[17] CHEN Q, FOLLY K A. Application of Artificial Intelligence for EV Charging and Discharging Scheduling and Dynamic Pricing: A Review[J]. Energies,2022,16(1)

[18]HU D E, LI Z C, PENG Y G, et al. Deep reinforcement learning for distribution networks with electric vehicle charging piles active reactive coordinated voltage control strategy [J]. Power system technology, 1-11[2023-02-14]

[19]LI H, LI G J, WANG K Y. Real-time dispatch strategy for electric vehicles based on deep reinforcement learning [J]. Automation of electric power systems, 2020, 44(22): 161-167
[21]Pecan Street Inc. Pecan Street[DB/OL].https://dataport.cloud/
[22]XU T,HUANG L,LI M L, ZHU M J.Research on portrait method of residential users based on multi-dimensional fine-grained behavior data[J]. Power Demand Side Management, 2019,21(03):47-52+58.
[23]FENG H X. Study on the demand response capability and customized DR contracts of Electric Vehicle Users based on historical charging data[D],North China Electric Power University,2021.
[24]HU J J,MA W S,XUE Y S,YAO L,XIE D L. Quantification of Reserve Capacity Provided by Electric Vehicle Aggregator Based on Framework of Cyber-Physical-Social System in Energy[J], Automation of Electric Power Systems, 2022,46(18):46-54.
[25] Kleinberg M R , Miu K , Chiang H D .Improving Service Restoration of Power Distribution Systems Through Load Curtailment of In-Service Customers[J]. Power Systems, IEEE Transactions on, 2011, 26(3):1110-1117.
[26] ZHANG C,FENG Z N,DENG S P,JIA C J,LU S. Multi-Energy Complementary Collaborative Peak-Load Shifting Strategy Based on Electro-Thermal Hybrid Energy Storage System[J]. Transactions of China Electrotechnical Society, 2021,36(S1):191-199.

[27] Ponnam V , Swarnasri K . Multi-Objective Optimal Allocation of Electric Vehicle Charging Stations in Radial Distribution System Using Teaching Learning Based Optimization[J]. International Journal of Renewable Energy Research, 2020, 10(1):366-377.
[28] FU G J,CAO,X. Research on Micro Grid Modeling and Economic Operation Optimization with CCHP and Energy Storage[J]. Journal of Jilin University (Information Science Edition), 2022,40(03):339-346.
[29] Polaris Power Exhibition Network.2December 2022 power purchase prices announced for grid agents across the country [EB/OL]. http://ex.bjx.com.cn/html/20221129/42218.shtml
[30] Polaris Solar PV Network. U.S. PV power purchase price as low as RMB 0.13 - 0.22 Yuan/kWh [EB/OL]. https://guangfu.bjx.com.cn/news/20190508/979088.shtml
[31]LI M L.Economic dispatch of power sysyem considering scenery power output prediction error[D].Yanshan University,2017.

8.2. Conference Paper

[13] AMROEN C, DECHANUPAPRITTA S. Coordinated control of battery energy storage system and plug-in electric vehicles for frequency regulation in smart grid [C]//2019 IEEE PES GTD Grand International Conference and Exposition Asia (GTD Asia), March 19-23, 2019, Bangkok, Thailand: 286-291

[20] YUAN H, LAI H, WANG Y, et al. Reserve capacity prediction of electric vehicles for ancillary service market participation [C]//2021 IEEE 2nd China International Youth Conference on Electrical Engineering (CIYCEE), Chengdu, China, 2021, 1-7

9. Appendices

Table A1 The value of power purchase from the main network at each moment of the microgrid day

Times	Load active power /kW	Load reactive power /kVar	PV reactive power /kVar	PV active power /kW	Purchase volume /kWh
1	4673.091	2893.165	0	0	1168.273
2	4655.04	2881.990	0	0	1163.76
3	4656.981	2883.192	0	0	1164.245
4	4485.345	2776.930	0	0	1121.336
5	4525.221	2801.617	0	0	1131.305
6	4374.378	2708.229	0	0	1093.594
7	4351.539	2694.089	0	0	1087.885
8	4353.417	2695.252	0	0	1088.354
9	4418.235	2735.381	0	0	1104.559
10	4295.808	2659.585	0	0	1073.952
11	4330.992	2681.368	0	0	1082.748
12	4325.055	2677.692	0	0	1081.264
13	4227.378	2617.219	0	0	1056.844
14	4361.838	2700.465	0	0	1090.46
15	4332.165	2682.094	0	0	1083.041
16	4231.152	2619.556	0	0	1057.788
17	4257.234	2635.703	0	0	1064.309
18	4247.94	2629.949	0	0	1061.985
19	4120.431	2551.007	0	0	1030.108
20	4159.812	2575.388	0	0	1039.953
21	4413.111	2732.209	0	0	1103.278
22	4393.698	2720.190	0	0	1098.425
23	4391.838	2719.038	0	0	1097.96
24	4431.963	2743.880	0	0	1107.991
25	4450.146	2755.137	0	0	1112.536

Times	Load active power /kW	Load reactive power /kVar	PV reactive power /kVar	PV active power /kW	Purchase volume /kWh
26	4719.048	2921.618	0	0	1179.762
27	4681.68	2898.483	0	0	1170.42
28	4630.017	2866.498	0	0	1157.504
29	4547.478	2815.397	6.080	9.12064	1134.589
30	4816.365	2981.868	69.704	104.556	1177.952
31	4950.012	3064.610	231.187	346.781	1150.808
32	4836.816	2994.529	493.023	739.535	1024.32
33	5139.501	3181.925	798.000	1197	985.6251
34	5249.139	3249.803	1108.883	1663.32	896.4537
35	5411.889	3350.564	1130.203	1695.3	929.1461
36	5318.397	3292.682	1298.039	1947.06	842.8347
37	5492.73	3400.614	1302.771	1954.16	884.6433
38	5519.769	3417.354	1132.097	1698.15	955.4058
39	5666.37	3508.116	891.427	1337.14	1082.307
40	5651.022	3498.614	970.541	1455.81	1048.803
41	5732.016	3548.758	1267.462	1901.19	957.7056
42	5965.563	3693.350	1192.328	1788.49	1044.268
43	6158.361	3812.714	1098.358	1647.54	1127.706
44	6110.763	3783.245	1059.051	1588.58	1130.547
45	6161.841	3814.868	1238.563	1857.84	1075.999
46	6139.911	3801.291	1205.459	1808.19	1082.931
47	5932.419	3672.830	1354.895	2032.34	975.0191
48	5757.306	3564.416	1359.541	2039.31	929.4985
49	5553.801	3438.423	1359.161	2038.74	878.7648
50	5558.157	3441.120	1395.184	2092.78	866.3453
51	5568.852	3447.742	1454.411	2181.62	846.809
52	5589.459	3460.499	1646.726	2470.09	779.8423
53	5603.259	3469.043	1837.044	2755.57	711.9232
54	6564.411	4506.903	1690.377	3835.57	680.2525
55	5632.773	3487.316	1715.552	2573.33	764.8611
56	5854.008	3624.285	1790.462	2685.69	792.0787
57	5821.8	3604.345	1863.250	2794.88	756.7312
58	5767.047	3570.446	1878.717	2818.08	737.2428
59	5577.306	3452.976	1901.600	2852.4	681.2264
60	5764.299	3568.745	1999.213	2998.82	691.37
61	5710.827	3535.640	2064.333	3096.5	653.5818
62	5766.393	3570.041	2257.615	3386.42	594.9927
63	5732.928	3549.323	2339.251	3508.88	556.0128
64	5744.817	3556.683	2321.301	3481.95	565.7164
65	5798.013	3589.618	2401.095	3601.64	549.0926
66	5921.064	3665.800	2477.725	3716.59	551.119
67	5912.895	3660.742	2281.510	3422.27	622.6573
68	6181.503	3827.041	2024.994	3037.49	786.0028
69	6277.113	3886.234	1749.518	2624.28	913.2089
70	6254.493	3872.230	1465.216	2197.82	1014.167
71	6330.936	3919.557	1161.708	1742.56	1147.093
72	6276.726	3885.994	850.366	1275.55	1250.294
73	6333.921	3921.404	538.744	808.116	1381.451
74	6136.494	3799.175	273.548	410.322	1431.543
75	6230.163	3857.167	86.313	129.469	1525.173
76	6196.275	3836.186	8.509	12.7632	1545.878
77	6080.7	3764.633	0	0	1520.175
78	6154.323	3810.213	0	0	1538.581
79	6074.385	3760.723	0	0	1518.596
80	6050.748	3746.089	0	0	1512.687
81	5979.825	3702.180	0	0	1494.956
82	6077.691	3762.770	0	0	1519.423
83	5979.264	3701.832	0	0	1494.816
84	5883.831	3642.749	0	0	1470.958
85	5866.917	3632.277	0	0	1466.729
86	5727.171	3545.759	0	0	1431.793
87	5586.657	3458.765	0	0	1396.664
88	5613.933	3475.652	0	0	1403.483
89	5332.452	3301.383	0	0	1333.113
90	5393.799	3339.364	0	0	1348.45
91	5173.353	3202.884	0	0	1293.338
92	5239.437	3243.797	0	0	1309.859
93	5073.954	3141.344	0	0	1268.488
94	4805.094	2974.890	0	0	1201.273
95	4719.582	2921.948	0	0	1179.895
96	4845.126	2999.674	0	0	1211.281